RAPID PUBLICATION

# Evidence of Subthalamic PGO-like Waves During REM Sleep in Humans: A Deep Brain Polysomnographic Study

Julio Fernández-Mendoza, MSc[1,2]; Beatriz Lozano, MD[3]; Fernando Seijo, MD[4]; Elena Santamarta-Liébana, MD[5]; Maria José Ramos-Platón, PhD[1]; Antonio Vela-Bueno, MD[2]; Fernando Fernández-González, MD[3]

*[1]Department of Psychobiology, School of Psychology, Universidad Complutense, Madrid, Spain; [2]Department of Psychiatry, School of Medicine, Universidad Autónoma, Madrid, Spain; Departments of [3]Clinical Neurophysiology, [4]Neurosurgery, and [5]Radiology II, Hospital Universitario Central de Asturias, Oviedo, Spain*

**Study Objectives:** The aim of this study was to examine whether the subthalamic nucleus (STN) plays a role in the transmission of PGO-like waves during REM sleep in humans.

**Design:** Simultaneous recordings from deep brain electrodes to record local field potentials (LFPs), and standard polysomnography to ascertain sleep/wake states.

**Setting:** Main Hospital, department of clinical neurophysiology sleep laboratory.

**Participants:** 12 individuals with Parkinson's disease, with electrodes implanted in the STN; and, as a control for localization purposes, 4 cluster headache patients with electrodes implanted in the posterior hypothalamus.

**Interventions:** All subjects underwent functional neurosurgery for implantation of deep brain stimulation electrodes.

**Results:** Sharp, polarity-reversed LFPs were recorded within the STN during REM sleep in humans. These subthalamic PGO-like waves (2–3 Hz, 80–200 μV, and 300–500 msec) appeared during REM epochs as singlets or in clusters of 3–13 waves. During the pre-REM period, subthalamic PGO-like waves were temporally related to drops in the submental electromyogram and/or onset of muscular atonia. Clusters of PGO-like waves occurred typically before and during the bursts of rapid eye movements and were associated with an enhancement in fast (15–35 Hz) subthalamic oscillatory activity.

**Conclusion:** Subthalamic PGO-like waves can be recorded during pre-REM and REM sleep in humans. Our data suggest that the STN may play an active role in an ascending activating network implicated in the transmission of PGO waves during REM sleep in humans.

**Keywords:** Basal Ganglia, subthalamic nucleus; REM sleep; PGO waves; fast oscillations; deep brain stimulation

**Citation:** Fernández-Mendoza J; Lozano B; Seijo F; Santamarta-Liébana E; Ramos-Platón MJ; Vela-Bueno A; Fernández-González F. Evidence of subthalamic PGO-like waves during REM sleep in humans: a deep brain polysomnographic study. *SLEEP* 2009;32(9):1117-1126.



RAPID EYE MOVEMENT (REM) SLEEP IN HUMANS IS CHARACTERIZED BY PERIODS OF LOW-VOLTAGE, MIXED-FREQUENCIES ELECTROENCEPHALOGRAM (EEG activation) with occasional sawtooth waves, rapid eye movements (REMs), and muscular atonia.[1] In cats, REM sleep is characterized by biphasic, sharp field potentials, called ponto-geniculo-occipital (PGO) waves, which are usually recorded in the lateral geniculate nucleus (LGN) of the thalamus.[2] These potentials, which can occur as an isolated event independently of eye movements or in clusters closely related to the bursts of REMs,[3] are associated with changes in the electromyogram (EMG)[4,5] and with synchronized cortical fast oscillations.[6,7] Although the original term "PGO waves" indicated their presence in the feline geniculostriate visual pathway, PGO-like waves largely transcend this sensory system and are disseminated throughout many nuclei and cortical areas of cats, such as other thalamic nuclei, cerebellum, oculomotor nuclei, cingulate gyrus, amygdala, and hippocampus.[2]

Although the vast majority of evidence regarding the existence of PGO waves comes from experiments in cats, some studies have suggested a human equivalent using a variety of methods: scalp,[8] cortical,[9] and pontine[10] electroencephalographic recordings; dipole tracing[11]; standardized low resolution brain electromagnetic tomography (sLORETA)[12]; positron emission tomography (PET)[13,14]; functional magnetic resonance imaging (fMRI)[15,16]; and magnetoencephalography (MEG).[17] However, studies that have systematically recorded deep brain structures during sleep to directly detect PGO-like waves in humans are lacking.

Functional neuroimaging studies of humans in REM sleep have shown a strong activation of the limbic and paralimbic regions of the forebrain, of the basal ganglia, and of the dorsal mesencephalon and pontine tegmentum.[18-20] In cats, PGO waves have been shown to originate in the mesopontine tegmentum and the cholinergic neurons of the pedunculopontine tegmental nucleus (PPN), which is located at the junction between the mesencephalon and the pons, representing the final common path for their transfer to thalamocortical systems.[2,21] The PPN and the basal ganglia have reciprocal projections involved in motor control, postural muscle tone, saccadic eye movements, and sleep.[22-27] Indeed, the PPN strongly modulates the neuronal activity of the subthalamic nucleus (STN), one of the core nuclei of the basal ganglia.[22,28] Because the basal ganglia are in a position to gate the transfer of information from the PPN to the thalamus and forebrain, investigators have proposed that during REM sleep, these nuclei may participate in an ascending activating network involved in the rostral transmission of PGO waves.[18,29]

**Submitted for publication January, 2009**
**Submitted in final revised form May, 2009**
**Accepted for publication June, 2009**

Address correspondence to: Fernando Fernández-González, MD, Department of Clinical Neurophysiology, Hospital Universitario Central de Asturias, c/ Julián Clavería s/n, 33006, Oviedo, Asturias (Spain); Tel: +34985107871; E-mail: fgfernando@msn.com

Renewed interest in deep brain stimulation (DBS) has led to efforts to record neuronal activity, in the form of local field potentials (LFP), directly from the STN in human individuals with Parkinson's disease following implantation of DBS electrodes.[30] Using simultaneous polysomnography (PSG) and DBS electrode recordings, the present study was designed to explore the participation of the STN in an ascending activating network involved in the transmission of PGO-like waves during REM sleep in humans.

## METHODS

### Subjects

Twelve patients with PD (6 men, 6 women) implanted with bilateral subthalamic DBS electrodes participated in the present study. Their mean age was 58.1 ± 8.92 years (range 42–73 years), and they had a mean disease duration of 12.5 ± 4.17 years (range 6–20 years), and a mean levodopa (L-dopa) treatment duration of 5.00 ± 2.68 years. These subjects were selected from an initial population of 48 patients of our 2003–2005 surgical period[31] who were simultaneously recorded with standard polysomnography (PSG) and DBS electrodes during nighttime sleep after 84 hours of DBS electrode implantation.[32] Patients from that group were included in the present study if they showed the following: (1) absence of complications for 6 days after surgical implantation; (2) positive localization of the DBS electrodes within the STN in both hemispheres, as assessed by postsurgical MRI, computed tomography (CT), and neurophysiologic recordings; and (3) an excellent clinical outcome after 1 year of subthalamic DBS. An excellent clinical outcome was defined as a significant reduction in L-dopa dose from the time of surgery to 1-year follow-up (960 ± 259.42 mEq/day *vs.* 227.27 ± 204.16 mEq/day; $t_{11} = 7.06$; P = 0.00004) and a significant increase in the following parameters: quality of life score (20 ± 6.32 *vs.* 7.08 ± 4.46; $t_{11} = 5.23$; P = 0.0003), based on the Unified Parkinson's Disease Rating Scale-part II (UPDRS II); motor disability score, based on the UPDRS III (40.92 ± 7.62 *vs.* 14.08 ± 6.44; $t_{11} = 12.89$; P = 0.00005); Hoehn and Yahr stage (3.33 ± 0.49 *vs.* 2.17 ± 0.33; $t_{11} = 9.11$; P = 0.00002); and scores on the Schwab and England scale (48.18 ± 18.34 *vs.* 86.82 ± 11.46; $t_{11} = -7.16$; P = 0.00003). These requirements for clinical outcome served to ensure the positive bilateral STN positioning of the DBS electrodes and to reduce the inter-individual variability in terms of DBS electrode positioning.[33] Four patients, who fulfilled these criteria were not selected: 2 did not show REM sleep during the nighttime recording, one asked to abort the sleep recording in the middle of the night, and the EMG for one patient was missing for more than half the PSG recording. The remaining 32 PD patients did not strictly fulfill the above criteria and were excluded from further analyses.

Four patients with cluster headache (CH; 3 men and 1 woman) implanted with unilateral DBS electrodes within the posterior hypothalamus during our 2005–2008 surgical period were also recorded with PSG. This allowed us to compare the REM sleep-related PGO-like activity in the STN recordings of PD subjects with recordings made near to, but clearly outside, the STN. The mean age of these subjects was 47.25 ± 2.63 years (range 45–50 years), and they had a mean disease duration of 16.25 ± 16.15 years (range 2–37 years).

All subjects provided written informed consent. The study protocol conformed to the Declaration of Helsinki and was approved by the Committee on Clinical Ethics at Hospital Universitario Central de Asturias (Oviedo, Asturias, Spain).

### Surgical and Neuroimaging Procedures

Individual target coordinates for implantation of DBS electrodes in the STN were calculated based on indirect neuroimaging methods combining CT and MRI, and were anatomically defined as 12 mm lateral to the anterior-commissure/posterior-commissure (AC-PC) midline, 2 mm behind the mid-commissural point, and 3 mm below the axial AC-PC plane. In order to improve the localization of the STN, intraoperative monitoring (IOM) of multiunitary neuronal activity was performed. An Ohye's semi-microelectrode was inserted along a pre-defined trajectory through a cranial burr-hole in patients under local anesthesia.[34] The insertions were made in steps of 1 mm, and the multiunitary activity was amplified, filtered, and displayed both as crude and 2-sec integrated signals. The latter was displayed over an anatomical atlas plane to indicate the trajectory, which typically was: caudate, thalamic reticularnucleus, internal capsule, top and bottom of the STN, and substantia nigra parsreticulata (SNr).[35] The STN was identified by the presence of an abrupt increase in the synchronization of crude multiunitary activity in the 15–35 Hz frequency band[36] with occasional discharges of ripples (> 200 Hz). When these activities were indicative of STN, wake subthalamic-related somatotopic responses to passive contralateral movements were performed.[36]

When IOM showed an atypical STN trajectory, median nerve evoked potentials were performed in order to detect ventroposterolateral thalamic and/or lemniscal activity. In addition, electrical monopolar stimulations through the macro-contact of the semi-microelectrode were used to detect undesirable motor responses, such as tonic or clonic contractions.[37] In the 24 hemispheres of the PD subjects, a mean number of 4.25 ± 1.31 trajectories were performed to ensure optimal placement. The best trajectory was used for implanting the DBS electrodes (Model 3389, Medtronic, USA). These electrodes had 4 cylindrical contacts with a length of 1.5 mm, a diameter of 1.5 mm, and a surface area of 6 $mm^2$. The contacts were spaced at a distance of 0.5 mm from one another, and were numbered 0, 1, 2, and 3 starting from the tip of the electrode. To ensure the accurate positioning of contact 2, insertions in steps of 1 mm were monitored using bipolar LFP recording, which was analyzed and displayed as described in the multiunitary detection of the STN. The goal of this approach was to position contact 2 in the dorsolateral area of the STN.[38] The final Cartesian coordinates for contact 2 of the DBS electrodes, calculated by integrating immediate postoperative MRI coordinates and intraoperative neurophysiological coordinates[39] were 11.96 ± 1.02 mm lateral to the AC-PC midline (X), −0.60 ± 2.35 mm behind the mid-commissural point (Y) and −3.49 ± 0.81 mm below the axial AC-PC plane (Z).

The same methodology was used for the implantation of unilateral hypothalamic DBS electrodes in the 4 CH subjects. First, the coordinates of the anterior border of the left STN were targeted using the same IOM methodology described above. Second, these coordinates were modified by moving 6 mm me-

dially in order to target the left posterior hypothalamus. The final Cartesian coordinates for contact 2 of the DBS electrodes were 5.97 ± 0.63 mm lateral to the AC-PC midline (X), −0.77 ± 0.22 mm behind the mid-commissural point (Y) and −0.92 ± 0.55 mm below the axial AC-PC plane (Z).

For a 6-day period following placement of DBS electrodes, the PD subjects remained ON dopaminergic medication and OFF DBS condition ("ON/OFF"), and the leads from each of the 4 contacts of the quadripolar DBS electrode were led out through the scalp and connected to external amplifiers for recording or stimulation purposes. Beginning 84 hours after implantation surgery, recordings of oculomotor, facial and brachial extensor motor responses evoked by subthalamic stimulation and somatosensory evoked potentials were performed. These recordings were used to assess the final positioning of the DBS electrodes with respect to the oculomotor nucleus, posterior thalamus, red nucleus, and cerebral peduncle. Also beginning at 84 hours post-surgery, standard wake video-EEG was performed in order to detect critical phenomena and possible postsurgical complications. The evoked responses and the EEG recordings were made following standard guidelines and methodologies for PD patients.[38]

### Simultaneous Deep Brain and Polysomnographic Recordings

Simultaneous standard nighttime PSG and bilateral subthalamic DBS electrode recordings were made the night after these postsurgical neurophysiologic evaluations and were carried out from 22:00 (lights off) until 08:00 (lights on). The behavioral state was monitored by video in real time. All PD subjects were on standard postsurgical medication: L-dopa (750 mg), phenytoin (300 mg), and cefazolin (3 g). Opiate medication was not administered to any of the PD subjects. Standard PSG derivations of EEG (C3-A2, C4-A1, O1-A2, and O2-A1), EOG (E1-A2, E2-A2), submental EMG, EKG, breathing, $SpO_2$, pulse, and body position were recorded in order to allow sleep staging. Subthalamic LFPs were recorded using the contacts of the DBS electrodes as bipolar derivations, numbered 0-1, 1-2, and 2-3. Subthalamic bipolar derivations were preferred, since we wished to ensure that the signals analyzed were as focally generated as possible and thus related to activity within the STN. These recordings were performed with a NicoletOne digital video-electroencephalograph. The PSG and STN signals were obtained by sampling the unfiltered data (DC 1 kHz) at 256 Hz (in recordings made before 2004) and at 512 Hz (in recordings made after 2004). These notch-filtered (50 Hz) records were displayed and scored as discrete 30-s epochs, with a sensitivity deflection of 70 μV/mm for scalp EEG and EOG, 50 μV/mm for EMG, and 20 μV/mm for STN derivations. A vascular artifact was recorded in the STN derivations during sleep; thus in all figures, the EKG and pulse derivations are displayed. Finally, 36 h after the PSG recording, the leads were internalized and connected to a permanently implanted programmable stimulator (Itrel model 3625, Medtronic, USA). This rendered the leads of the DBS electrodes inaccessible until the replacement of the stimulator's battery (after approximately 5 years of DBS).

DBS requires adjustment of the most effective DBS electrode contact, as well as modification of stimulation parameters and dopaminergic medication in order to manage possible adverse effects. Therefore, at 1-year follow up, when the subjects' postsurgical clinical courses had stabilized, 2 clinical neurologists performed double-blind, video-based evaluations using the standard clinical scales described above. Based on these evaluations, at 1-year follow-up for the 12 PD subjects studied here, 16 hemispheres were receiving the originally intended monopolar stimulation with contact 2, seven were receiving monopolar stimulation with contact 1, and only one was receiving monopolar stimulation with contact 3. These data confirm that the STN was successfully targeted in the vast majority of hemispheres.

### Data Analyses

Sleep stage scoring was performed blind to the STN traces according to standard methods.[36] However, it was difficult to score NREM sleep stage 3 following the standard criteria (i.e., ≥ 20% of a 30-s epoch consisting of waves of peak-to-peak amplitude > 75 μV and 0.5–2 Hz frequency recorded in scalp EEG),[40] probably because of the acute postsurgical condition of the subjects (e.g., bilateral frontal burr-holes, contusion, and pneumoencephalus). Thus, 30-s epochs were scored as wakefulness; NREM stages 1 and 2, with the latter including those epochs that did not strictly fulfill the standard criteria for stage 3; and REM sleep. After scoring sleep stages, 2 researchers visually analyzed the STN traces during all epochs, displaying them with a low band-pass filter of 1 Hz and a high band-pass filter of 100 Hz. For all analyses, the first REM sleep period of the last third of the total sleep time (TST) was selected because REM sleep episodes are longer during the last third of the night.[1] We defined pre-REM as the 3 epochs (90 s) preceding the first epoch scored as REM sleep.[40]

Subthalamic PGO-like waves were analyzed in terms of amplitude, frequency, duration, polarity reversal, organization, density, and length of the inter-potential interval (IPI). To assess the bilateral (inter-hemispheric) synchrony of PGO-like waves, we used the interval between the peak of the left PGO-like wave and that of the right one in each patient (n = 180 intervals) to calculate the mean consecutive difference (MCD). The association between subthalamic PGO-like waves and REMs was analyzed by calculating the incidence of PGO-like waves 500 ms before and after the EOG deflection.

Synchronized oscillations in the STN traces were analyzed using digital filtering to group δ (0.5–4 Hz), θ (4–8 Hz), α (8–12 Hz), σ (12–15 Hz), and β (15–35 Hz) frequency bands. While some authors have suggested that there is no reason to split fast oscillations into β (15–30 Hz) and γ (> 30 Hz) categories in order to reflect different functional states,[7] studies of the robust β oscillatory activity of the STN in healthy rats, nonhuman primates, and PD patients[30] suggest that fast oscillations in the β band are important for motor processing.[30,41-43] In fact, these fast oscillations are considered a hallmark of the STN.[30] Thus, the study of fast oscillations in the 15–35 Hz range allowed us to be consistent with previous STN studies,[30,42,43] to avoid the possible confounder of subthalamic < 15 Hz spindle-like activity,[7] and to avoid possible changes in subthalamic > 40 Hz oscillations induced by postsurgical L-dopa treatment.[30,41] Subthalamic β oscillations were analyzed in relation to the clusters of PGO-like waves by displaying the raw subthalamic signal and the

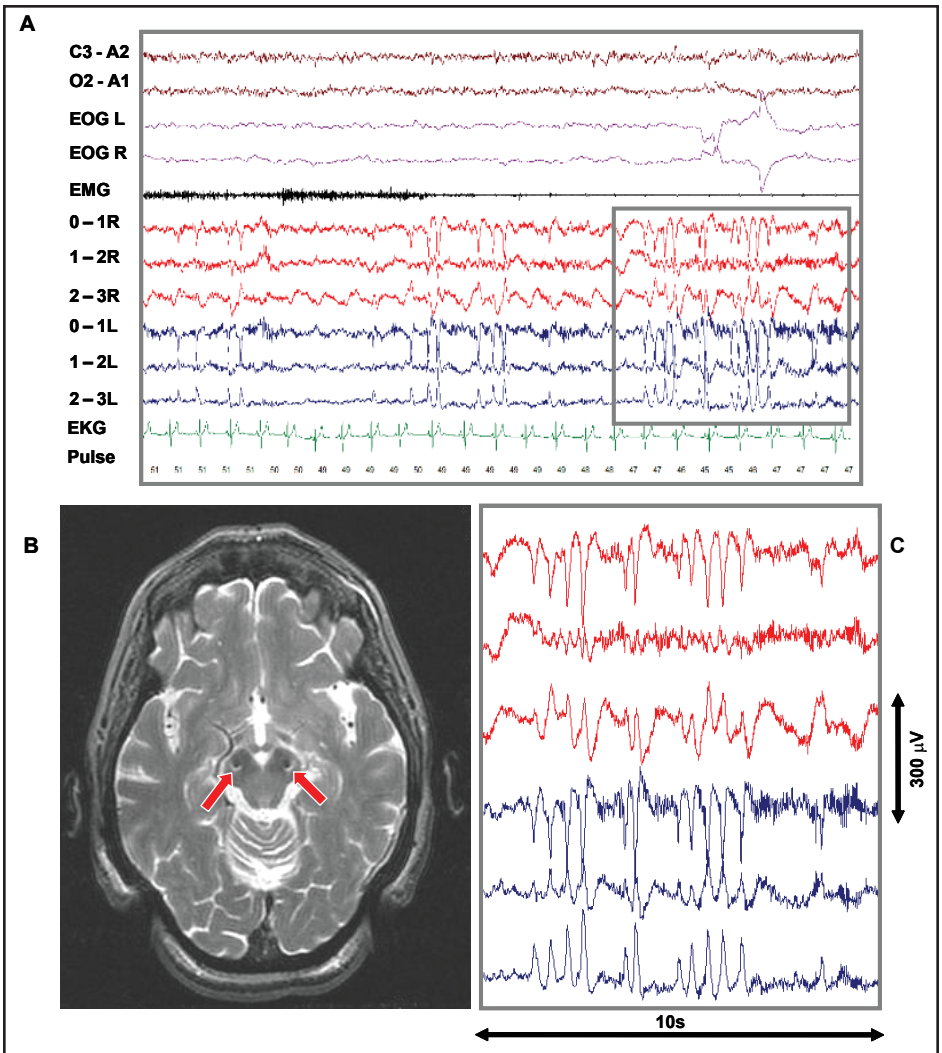


**Figure 1**—REM sleep related subthalamic activity. **(A)** A 30-s epoch of simultaneous PSG and bipolar subthalamic recording showing the pattern of PGO-like waves. A 0.5–100 Hz band-pass filter reveals the vascular pulse component in the right 2-3 derivation. **(B)** Axial MRI view showing DBS electrodes at the level of contact 0. **(C)** Enlarged section of the pattern of subthalamic PGO-like waves recorded during REM sleep.

filtered one, together with the standard PSG derivations. For visual analyses, low-β (15–25 Hz) and high-β (25–35 Hz) frequency bands were also displayed. The power of subthalamic 15–35 Hz activity before, after, and during the clusters of PGO-like waves was analyzed statistically.

### Statistical Analyses

Paired Student *t*-tests were used to analyze changes in mean clinical and pharmacological parameters at 1-year follow-up, and changes in the power of the β band before and after the clusters of PGO-like waves. Student *t*-tests were used to analyze mean differences between subthalamic and hypothalamic subjects in terms of the Cartesian coordinates of contact 2 of the DBS electrodes. A repeated-measures ANOVA with Tukey HSD post hoc multiple comparisons was used to analyze mean changes in β power before, during, and after the PGO-like clusters. Linearity of the increase in β power associated with PGO-like clusters was tested with polynomial analysis. Effect size was measured with the partial eta-squared statistic ($_p\eta^2$). Parametric tests were used because data were normally distributed (Kolmogorov-Smirnov tests, $P > 0.10$), and because these tests are robust to violations of their assumptions and to the loss of power incurred by the use of the equivalent nonparametric tests. The significance level was set at $P \leq 0.05$ (corrected for multiple comparisons).

## RESULTS

### PSG Characteristics of the Sample

The scoring of standard PSG recordings to ascertain sleep/wake states in the 12 PD subjects showed a mean sleep onset latency of 19.92 ± 19.63 min, and a mean TST of 394.88 ± 87.95 min. The percentages of sleep stages based on TST were 28.92% ± 17.61% for stage 1, 55.78% ± 20.43% for stage 2, and 15.30% ± 7.24% for REM sleep. Stage 3, as defined by current standard criteria,[40] was not scored (see Methods). The REM latency was 71.29 ± 79.59 min. The percentage of wakefulness after sleep onset (WASO) based on the time spent in bed was 26.68% ± 16.61%. Although these recordings reflected the well-known disturbed sleep architecture in PD,[44] the amount of sleep stages recorded was satisfactory for further analyses.

### Detection of Subthalamic PGO-like Waves

In all 24 hemispheres of the 12 bilaterally implanted subjects, a pattern of subthalamic sharp field potentials was detected during REM sleep (Figure 1). These LFPs were bilaterally synchronous (MCD = 4.06 ms; sampling precision: 1000/256 = 3.906 ms/sample; Figure 1d), showed polarity reversal at different contact levels of the DBS electrodes, and appeared as singlets/doublets or in clusters with a variable number of waves. During periods of WASO with REMs and NREM sleep (outside the pre-REM period), subthalamic PGO-like waves were not detected (data not shown).

### Characterization of Subthalamic PGO-like Waves

Two types of subthalamic sharp field potentials were found during full episodes of REM sleep. The first type (type I) consisted of those appearing in singlets or doublets that were not closely associated with the bursts of REMs, and were typically characterized by a duration of 366.89 ± 52.02 ms, an amplitude of 87.86 ± 27.64 µV, an IPI of 387.08 ± 64.50 ms, and a frequency of 2.66 ± 0.46 Hz (Figure 2a). The second type (type II) were those that appeared in clusters, with a density of 7.90 ± 2.13

waves/cluster, and that were strongly associated with the bursts of REMs, usually preceding them. These clusters typically had a duration of 366.52 ± 49.78 ms, an amplitude of 96.23 ± 22.57 μV, an IPI of 369.17 ± 61.65 ms, and a frequency of 2.79 ± 0.50 Hz (Figure 2a).

During pre-REM, subthalamic LFPs similar in amplitude, duration, and frequency to those that were found during REM sleep and that were classified as type I also occurred. These occasional pre-REM subthalamic potentials were associated with drops in submental EMG and with the onset of total submental EMG atonia (Figure 2b). Occasionally, clusters of PGO-like waves appeared during pre-REM; when they did, they were associated with the onset of muscular atonia and with certain degree of instability of the eyes recorded in the EOG (Figure 2c). Figure 3 shows the association of type I waves during pre-REM with drops in submental EMG and with onset of muscular atonia (Figure 3a), as well as the association of type II waves with REMs (Figure 3b). There was a higher incidence of PGO-like waves before the EOG deflection, specifically with peaks between −281 ms to −328 ms, between −94 ms and −117 ms, and also around the deflection, between 0 ms and +23 ms (Figure 3b). Since these waves typically last 366 ms and have an IPI of ~370 ms, approximately 2 waves occurred around the EOG deflection.

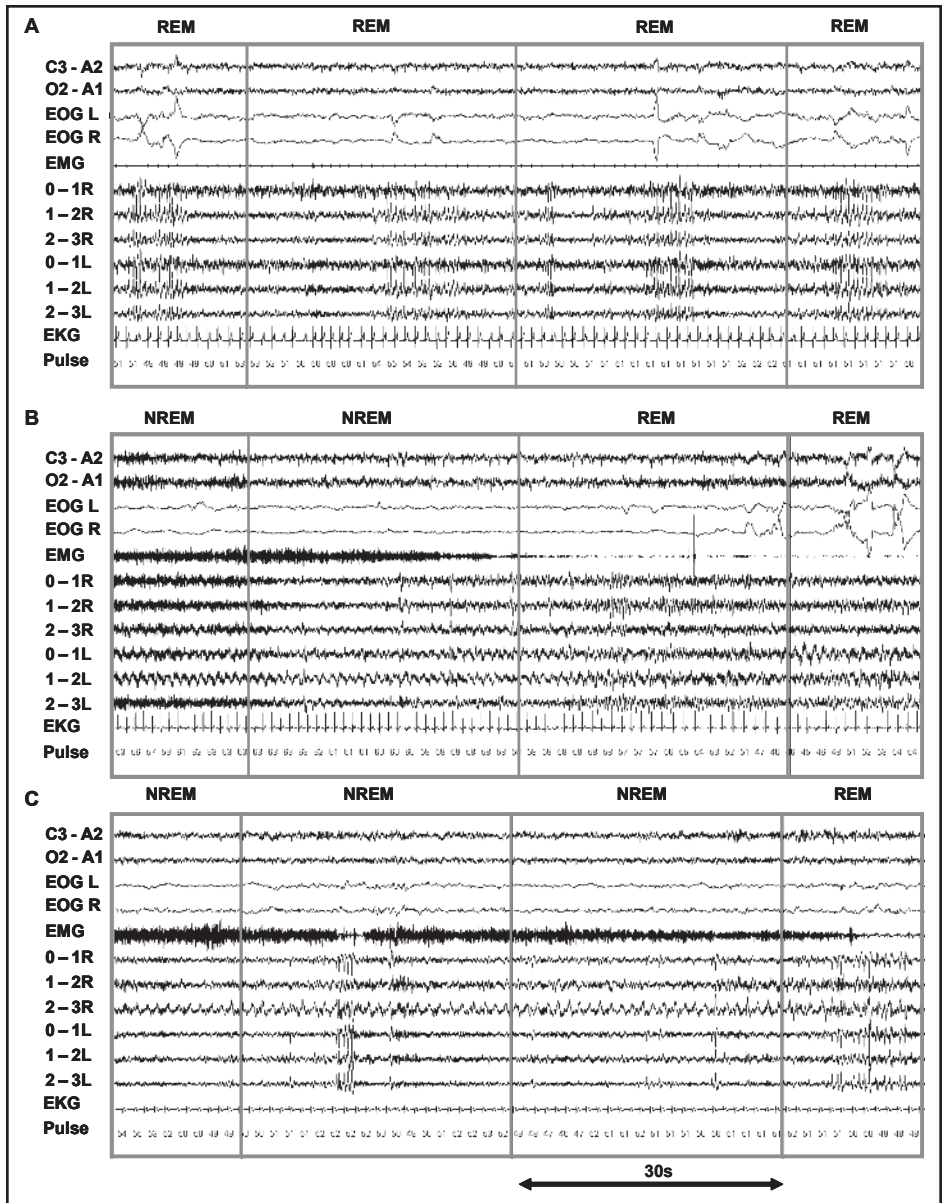


**Figure 2**—Sequences of pre-REM and REM sleep. **(A)** A 90-s REM sleep period showing the clusters of subthalamic PGO-like waves associated with REMs. **(B)** Fast transition to REM sleep from a pre-REM sleep period where subthalamic PGO-like waves appeared as singlets linked to drops in the EMG and to onset of definite muscular atonia. **(C)** Transition to REM sleep from a pre-REM sleep period, where a cluster of subthalamic PGO-like waves appeared associated with short-lasting total EMG atonia and instability of the eyes recorded in the EOG. All subthalamic traces band-pass filtered at 1–100 Hz.

### Location of Subthalamic PGO-like Waves

Subthalamic PGO-like waves showed polarity reversal, which is not expected for volume-conducted activity and which indicates a local field origin.[7,30] The specificity of this subthalamic activity was assessed by comparing these recordings with those made in the left posterior hypothalamus of CH subjects. The latter recordings showed sharp, non–polarity-reversed field potentials similar in shape to those found in the STN of PD subjects. Significant differences were detected in the Cartesian coordinates of contact 2 of the DBS electrodes between subthalamic PD subjects and hypothalamic CH subjects [final mediolateral (X), $t_{26} = 7.51$; P = 0.00006; dorsoventral (Z), $t_{26} = -6.08$; P = 0.0002] (see Methods for mean values). In contrast, no significant difference between these 2 groups was found in the final Cartesian rostrocaudal coordinate (Y) [$t_{26} = 3.71$; P = 0.714]. These data indicate that the recorded subthalamic PGO-like potentials had a local field origin within the STN, and that PGO-like waves can be recorded as volume-conducted potentials in the vicinity of the STN.

### Association of PGO-like Waves with Subthalamic Fast (15–35 Hz) Oscillations

Increased subthalamic β (15–35 Hz) activity during and after the clusters of subthalamic PGO-like waves (Figure 4a) was revealed by spectral analyses (Figure 4b). Zooms of subthalamic segments are displayed in Figure 4c to show the polarity reversal of these β oscillations.

Figure 4d shows the significant enhancement of β (15–35 Hz) power following the clusters of PGO-like waves (1.44 ± 0.90 $\mu V^2$ *vs.* 13.46 ± 8.12 $\mu V^2$; $t_{11} = 5.00$; P = 0.0004). Furthermore, the β power of each second after the occurrence of each PGO-like wave of the cluster was analyzed. Since all subjects

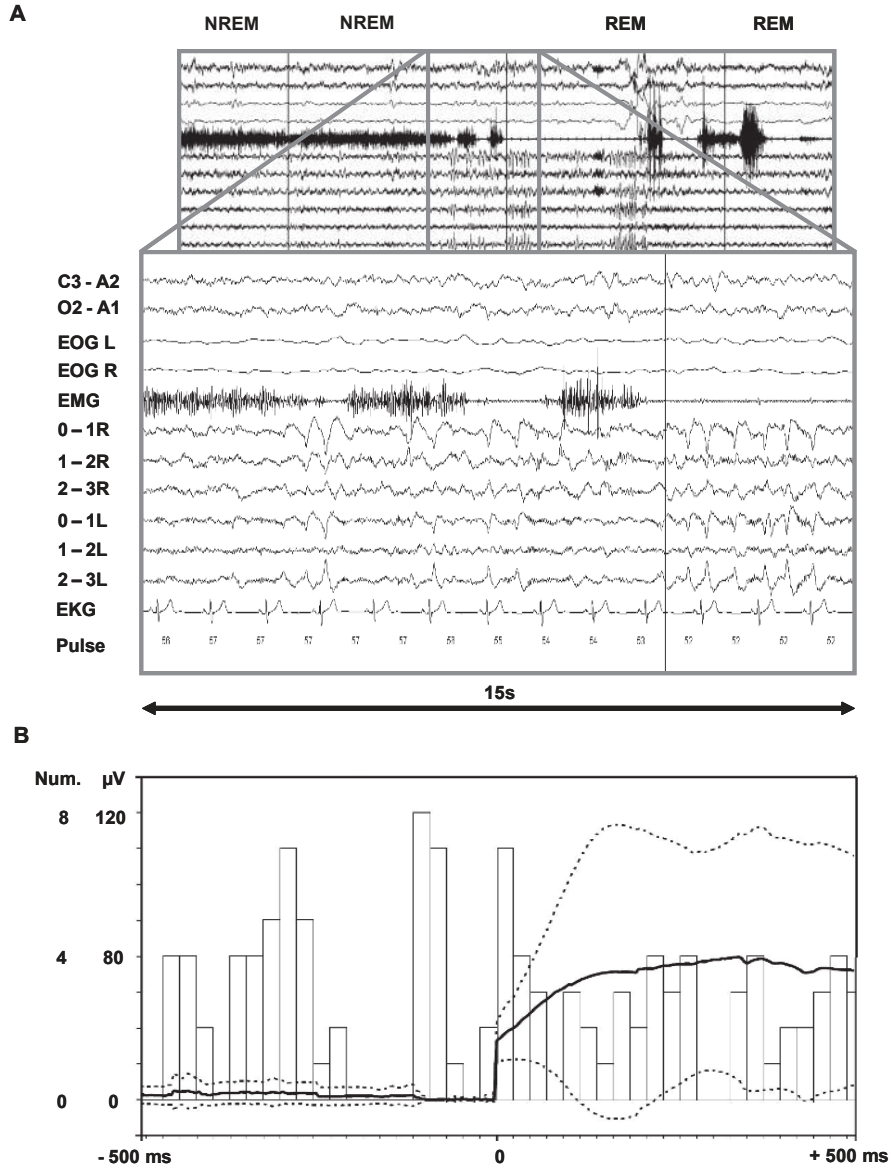


**Figure 3**—Subthalamic PGO-like waves, muscular atonia, and REMs. **(A)** A 15-s enlarged section of a pre-REM–REM sleep transition showing the close association of subthalamic PGO-like waves with drops in the EMG and the onset of muscular atonia during pre-REM sleep. Subthalamic traces band-pass filtered at 1–100 Hz. **(B)** Histogram showing the incidence of PGO-like waves 500 ms before and after REMs. The solid line represents the averaged amplitude deflection in the EOG (µV), and the dotted lines represent ± SD. Bars represent the incidence (num. = number) of PGO-like waves.

showed ≥ 6 waves per cluster during the first epoch of the REM episode, subsequent analyses were made on the β power before the cluster, after each wave in the cluster until the fifth wave, and after the cluster (i.e., the 6th wave in 3 subjects, and the 7,th 8th, and 9th in 1, 2, and 6 subjects, respectively). To examine within-subjects differences in β power associated with clusters of PGO-like waves, repeated-measures ANOVA was conducted ($F_{1,11} = 9.93$; P = 0.009; ${}_p\eta^2 = 0.475$).

Table 1 shows pairwise comparisons that revealed significant differences in the β power before the clusters and the β power after the third and subsequent PGO-like waves of the clusters. Figure 4e clearly shows a significant linear increase in β power during clusters of PGO-like waves ($F_{1,11} = 32.70$; P = 0.0001; ${}_p\eta^2 = 0.748$), with a peak occurring after the clusters (see Table 1). After we adjusted for age, disease duration, and medication, this increase remained significant, and the mean differences remained similar to those reported in Table 1.

## DISCUSSION

The main finding of this study was the identification in humans of a bilateral pattern of sharp field potentials within the STN that preceded and accompanied REM sleep and that resembled the PGO waves typically recorded in cats. These subthalamic PGO-like waves appeared as singlets or as clusters (2–3 Hz, 2–8 s, 3–13 waves per cluster) and were associated with drops in the EMG and with total muscular atonia, both during epochs of REM sleep and during epochs preceding it (pre-REM). Furthermore, clusters of subthalamic PGO-like waves were typically associated with the bursts of REMs and with an enhancement of subthalamic fast (15–35 Hz) oscillatory activity. Our data support the role previously proposed[18] for the basal ganglia nuclei as part of an ascending activating network involved in the rostral transmission of PGO waves during REM sleep in humans.

Many of the features of subthalamic PGO-like waves recorded as LFPs in the present study using DBS electrodes are consistent with those of previous studies in animals. Datta[2] has summarized the characteristics of naturally occurring feline PGO waves during REM sleep as biphasic, sharp field potentials that last 60–120 ms and have an amplitude of 200–300 µV. These potentials occur as singlets and as clusters containing a variable number of PGO waves (3–5 waves), with a density ranging from 30 to 60 waves/min. In the rat, pontine PGO-like waves have amplitudes (± 150 µV) and durations (± 100 ms) similar to those of PGO waves recorded in the cat.[2] The interspecies variability may be due to morphological differences, or to the type and/or the positioning of the electrodes used relative to the dipole source. Similar to what we observed in humans (Figure 2), PGO waves in the cat precede REM sleep by approximately 30 to 90 s, appearing as singlets that precede the other key signs of REM sleep (i.e., EEG activation, muscular atonia, and REMs), and they continue to occur as clusters throughout REM sleep.[2]

In the present study, as in studies of feline PGO waves,[2,3] singlet subthalamic PGO-like waves were independent of eye movement (type I), while clusters of PGO-like waves were typi-

**Table 1**—Enhancement of β (15–35 Hz) Power Associated with Clusters of Subthalamic PGO-like Waves

| | Beta Power[1] | 0. | 1. | 2. | 3. | 4. | 5. | 6. |
|---|---|---|---|---|---|---|---|---|
| 0. Before the cluster | 1.44 ± 0.26 | — | 0.9904 | 0.3910 | **0.0210** | **0.0432** | **0.0002** | **0.0001** |
| 1. After wave 1 | 2.82 ± 0.42 | — | — | 0.8362 | 0.1325 | 0.2276 | **0.0016** | 0.0001 |
| 2. After wave 2 | 5.36 ± 0.96 | — | — | — | 0.8468 | 0.9420 | 0.0771 | **0.0014** |
| 3. After wave 3 | 7.84 ± 1.77 | — | — | — | — | 0.9999 | 0.7060 | 0.0637 |
| 4. After wave 4 | 7.34 ± 1.21 | — | — | — | — | — | 0.5356 | **0.0320** |
| 5. After wave 5 | 10.82 ± 1.91 | — | — | — | — | — | — | 0.8086 |
| 6. After the cluster | 13.46 ± 2.34 | — | — | — | — | — | — | — |

[1]Values are means ± SEM $\mu V^2$; 0. = β power 1 s before the first wave of the cluster (i.e., 1.); 1. to 5. = β power 1s after each wave of the cluster in consecutive order; 6. = β power 1 s after the cluster (i.e., the 6th wave in 3 subjects and the 7th, 8th and 9th in 1, 2, and 6 subjects, respectively). Bold P-values are significant at the $P < 0.05$ level (corrected for multiple comparisons)

cally associated with the bursts of REMs during REM sleep (type II). Vanni-Mercier and Debilly[45] provided evidence for a parallel anatomical organization of the oculomotor and PGO systems in cats; these authors suggested that an interconnection between the PPN and the caudoventral pontine reticular formation (PRF) may operate as a common generator of REMs and PGO waves during REM sleep.[45] Indeed, a network involving the superior colliculus (SC), PPN, SNr, and STN, among other nuclei, has been suggested to generate waking saccades[46-48]; thus, an association between the subthalamic PGO-like clusters and the bursts of REMs during REM sleep is reasonable. It is possible that we failed to detect subthalamic PGO-like waves during periods of WASO with REMs either because different neurophysiological mechanisms subserve the generation of waking saccades and REM sleep saccades, or because the oculomotor system is in a different state of excitation during these different types of saccades.[49] This issue deserves further investigation in humans.

We also found that subthalamic PGO-like waves were associated with drops in the submental EMG and/or with the onset of muscle atonia. Previous studies in cats showed that naturally occurring and externally induced PGO waves are associated with the suppression of EMG during pre-REM and REM sleep periods.[4,5,50] Since PGO waves have been proposed to reflect central activation of alerting mechanisms,[51-53] a functional link has been suggested between the mechanisms involved in the generation of PGO waves and the inhibitory motoneuron system, which may serve to preserve atonia from potentially disruptive PGO-related influences.[5] Thus, it is possible that the same mechanism that in cats induces PGO waves, REMs, and the inhibition of motoneurons during REM sleep, drives the subthalamic PGO-like waves recorded in the present study.

Furthermore, cortical PGO waves have been shown to underlie the synchronization of cortical fast oscillations during REM sleep in cats.[6,7] During REM sleep in humans, cortical and subcortical fast oscillations are enhanced[54-56] and strong subthalamo-cortical coherence is observed in the β range.[30,56] Since PGO waves can not be clearly identified with scalp EEG in humans, studies have corroborated the synchronization of scalp fast oscillations as associated with the bursts of REMs.[57] In the present study, clusters of subthalamic PGO-like waves related to the time occurrence of the bursts of REMs were associated with an enhancement of the power of fast subthalamic oscillatory activity in the β (15–35 Hz) range. The linear increase in the power of subthalamic β oscillations provides evidence for the proposed role of PGO-like activity in the progressive synchronization of fast oscillations during REM sleep.

Current models of REM sleep posit that activation of the forebrain occurs through ascending activating systems in the brainstem reticular arousal system and the basal forebrain; this activation is aminergically deficient and cholinergically driven,[29] and it is modulated by GABAergic and glutamatergic release.[58] The cholinergic neurons of the PPN, which are the final common path of brainstem networks for the transfer of PGO waves to thalamocortical systems,[12,21] extensively innervate the STN, which, in turn, sends back glutamatergic projections to the PPN.[22-25] The STN is a key component of the basal ganglia and a potent regulator of the basal ganglia-thalamocortical associative and limbic circuits.[59] In fact, the output nuclei of the basal ganglia (SNr/internal Globus Pallidus, GPi), which send projections to the thalamocortical system, are modulated by three pathways: a "direct pathway" (cortico-striatal-SNr/GPi), an "indirect pathway" (cortico-striatal-external GP-STN-SNr/GPi) and a "hyperdirect pathway" (cortico-STN-SNr/GPi).[23] In wakefulness, these pathways are thought to be functionally involved in the execution and inhibition of movement, respectively.[24,30,47] Although little is known about how these anatomo-functional pathways operate during REM sleep,[25,60] some studies have reported that the basal ganglia output nuclei may play a role in the modulation of REM sleep phenomena; the precise role depends on their interconnections with the PPN.[23,26,27] Since previous authors have proposed that the PPN-STN projection is a key interface linking the basal ganglia pathways with brainstem systems involved in motor control, sleep, and arousal,[22-25,61] it is therefore plausible that, during REM sleep, the PPN drives the pattern of subthalamic PGO-like waves recorded in the present study.

PGO waves have been traditionally regarded as a physiological correlate of dreaming[29,62,63] and, recently, of sleep-dependent learning.[64] Moreover, changes in subthalamic β oscillations have been shown to be strongly associated with overt and imaginary movement.[42,43] Future studies should therefore examine how the pattern of subthalamic PGO-like waves and fast oscillations during REM sleep relate to these cognitive phenomena.

Admittedly, our observations are limited by several factors. First, we studied individuals with PD, a disease known to involve sleep pathology,[44] such as decreased REM sleep periods, REM density, and muscle atonia, as well as the presence of REM sleep behavior disorder (RBD). Nevertheless, none of the 12 PD individuals showed complex overt behaviors during

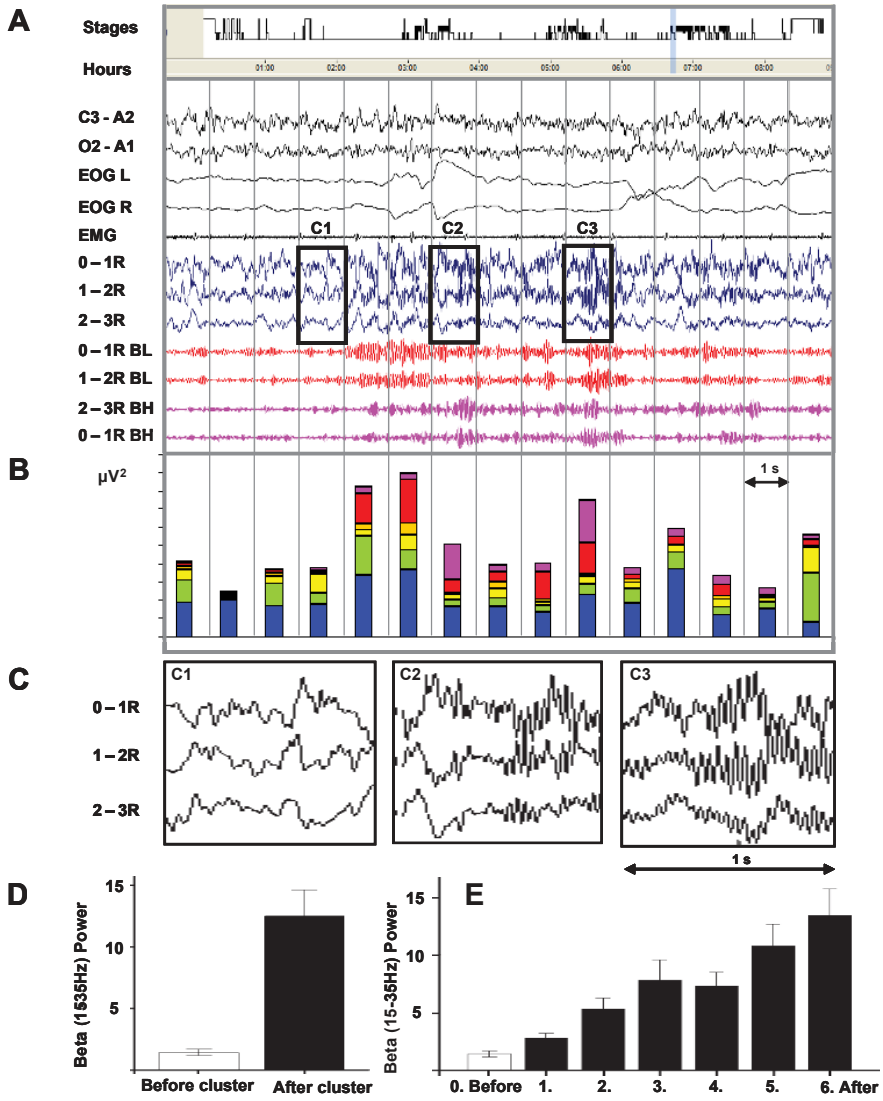


**Figure 4**—Subthalamic PGO-like clusters and fast (15–35Hz) oscillations. **(A)** A 15-s REM epoch of simultaneous PSG and STN traces from the period marked in light blue of the hypnogram (top). Subthalamic traces are displayed as raw (1–100 Hz), low-β (15–25 Hz; red) and high-β (25–35 Hz; pink) filtered derivations. Sawtooth waves in C3-A2 are temporally linked to subthalamic PGO-like waves. **(B)** Display of the fast Fourier transform (FFT) of 1-2R STN traces for different relative powers ($\mu V^2$) for each second of the epoch: blue = δ (0.5–4 Hz), green = θ (4–8 Hz), yellow = α (8–12 Hz), orange = σ (12–15 Hz), red = low-β (15–25 Hz), pink = high-β (25–35 Hz). **(C)** Enlarged sections (1 s) of raw subthalamic traces revealing reduced β (15–35 Hz) activity before the clusters (C1), and polarity-reversed β activity (C2) with a higher amplitude after the cluster (C3). **(D)** Histogram showing the significant increase in beta power after the clusters of subthalamic PGO-like waves. **(E)** Histogram showing the linear increase in β power during the clusters (see Table 1).

REM sleep, and none had been diagnosed with RBD. Moreover, our EOG (E1-A2, E2-A2) montage did not record the complete direction of REMs,[40] and in some cases only certain degree of instability of the eyes could be recorded; this may have affected the REM density recorded and thus the association of PGO-like waves with REMs. Second, we recognize that the synchronization in the PGO-like and β bands may reflect the pathological hyperactivity of the STN in PD, which is characterized by an augmented synchrony and a mildly increased firing rate with bursting activity.[30] It is therefore possible that PGO-like and β activities are more evident within the STN due to this tendency towards higher neuronal synchrony in PD. However, the fact that we recorded non–polarity-reversed PGO-like waves in the vicinity of the STN of CH patients suggests that our results are valid. Future studies should use other pathological models of the STN and/or multi-target recordings (i.e., PPN+STN; PPN+GPi) in humans and other mammals. Third, the surgical implantation, the acute post-surgical state and/or drug therapy itself may have altered the normal dynamics of the activity within the STN. The neuronal shock and/or the edema may have altered the amplitude of the activities recorded. In fact, changes in L-dopa treatment have been shown to modify the frequencies recorded in the STN; however, these changes attenuate oscillations in the β band and enhance those in higher frequency bands.[30,41]

Notwithstanding these limitations, we conclude that subthalamic PGO-like waves can be recorded during pre-REM and REM sleep in humans. These sharp field potentials are associated with muscular atonia, with the bursts of REMs, and with an enhancement of subthalamic fast oscillatory activity. Our findings give further support to animal sleep research exploring the functional significance of PGO waves and its translation to humans.

## ACKNOWLEDGMENTS

The authors are grateful to Dr. Menéndez-Guisasola (R.I.P.) and Dr. Salvador-Aguiar for their expertise in neurological clinical work with PD patients. We thank A. Galindo, C. García, and E. de la Hoz for their technical assistance. We are also grateful to Dr. T.C. Wetter (Max Planck Institute of Psychiatry, Germany) and Dr. R. Wehrle (University of Zurich, Switzerland) for their comments on a previous version of this manuscript. JFM is supported by the Research Personnel Program of Complutense University (FPI/2006-2010).

## DISCLOSURE STATEMENT

This was not an industry supported study. The authors have indicated no financial conflicts of interest.

## REFERENCES

1. Carskadon MA, Dement WC. Normal human sleep: an overview. In: Kryger MH, Roth T, Dement WC eds. Principles and prac-

tice of sleep medicine. 4th ed. Philadelphia: Elsevier Saunders 2005:13-23.
2. Datta S. Cellular basis of pontine ponto-geniculo-occipital wave generation and modulation. Cell Mol Neurobiol 1997;17:341-65.
3. Morrison AR, Pompeiano O. Vestibular influences during sleep. IV. Functional relations between vestibular nuclei and lateral geniculate nucleus during desynchronized sleep. Arch Ital Biol 1966;104:425-58.
4. López-Rodríguez F, Chase MH, Morales FR. PGO-related potentials in lumbar motoneurons during active sleep. J Neurophysiol 1992;68:109-16.
5. Kohlmeier KA, López-Rodríguez F, Morales FR, Chase MH. Relationship between sensory stimuli–elicited IPSPs in motoneurons and PGO waves during cholinergically induced muscle atonia. J Neurophysiol 1997;78:2145-55.
6. Amzica F, Steriade M. Progressive cortical synchronization of ponto-geniculo-occipital potentials during rapid eye movement sleep. Neuroscience 1996;72:309-14.
7. Steriade M, Amzica F, Contreras D. Synchronization of fast (30–40 Hz) spontaneous cortical rhythms during brain activation. J Neurosci 1996;16:392-417.
8. McCarley RW, Winkelman JW, Duffy FH. Human cerebral potentials associated with REM sleep rapid eye movements: links to PGO waves and waking potentials. Brain Res 1983;274:359-64.
9. Salzarulo P, Lairy GC, Bancaud J, Munari C. Direct depth recording of the striate cortex during REM sleep in man: are there PGO potentials?. Electroencephalogr Clin Neurophysiol 1975;38:199-202.
10. Lim AS, Lozano AM, Moro E, et al. Characterization of REM-sleep associated ponto-geniculo-occipital waves in the human pons. Sleep 2007;30:823-7.
11. Inoue S, Saha UK, Musha T. Spatio-temporal distribution of neuronal activities and REM sleep. In: Mallick BN, Inoue S eds. Rapid eye movement sleep. New York: Marcel Dekker 1999:214-20.
12. Abe T, Ogawa K, Nittono H, Hori T. Neural generators of brain potentials before rapid eye movements during human REM sleep: a study using sLORETA. Clin Neurophysiol 2008;119:2044-53.
13. Hong CC, Gillin JC, Dow BM, Wu J, Buchsbaum MS. Localized and lateralized cerebral glucose metabolism associated with eye movements during REM sleep and wakefulness: a positron emission tomography (PET) study. Sleep 1995;18:570-80.
14. Peigneux P, Laureys S, Fuchs S, et al. Generation of rapid eye movements during paradoxical sleep in humans. Neuroimage 2001;14:701-8.
15. Wehrle R, Czisch M, Kaufmann C, et al. Rapid eye movement-related brain activation in human sleep: a functional magnetic resonance imaging study. Neuroreport 2005, 16:853-7.
16. Miyauchi S, Misaki M, Kan S, Fukunaga T, Koike T. Human brain activity time-locked to rapid eye movements during REM sleep. Exp Brain Res 2009;192:657-67.
17. Ioannides AA. MEG tomography of human cortex and brainstem activity in waking and REM sleep saccades. Cereb Cortex 2004;14:56-72.
18. Braun AR, Balkin TJ, Wesenten NJ, et al. Regional cerebral blood flow throughout the sleep-wake cycle. An H2(15)O PET study. Brain 1997;120:1173-97.
19. Nofzinger EA. Functional neuroimaging of sleep. Semin Neurol 2005;25:9-18.
20. Maquet P, Péters J, Aerts J, et al. Functional neuroanatomy of human rapid-eye-movement sleep and dreaming. Nature 1996;383:163-6.
21. Steriade M, Pare D, Datta S, Oakson G, Curro Dossi R. Different cellular types in mesopontine cholinergic nuclei related to ponto-geniculo-occipital waves. J Neurosci 1990;10:2560–79.
22. Mena-Segovia J, Ross HM, Magill PJ, Bolam JP. The pedunculopontine nucleus: towards a functional integration with the basal ganglia. In: Bolam JP, Ingham CA, Magill PJ eds. The basal ganglia VIII. Advances in behavioral biology; volume 56. New York: Springer Science and Business Media 2005:533-44.
23. Mena-Segovia J, Bolam JP, Magill PJ. Pedunculopontine nucleus and basal ganglia: distant relatives or part of the same family? Trends Neurosci 2004;27:585-8.
24. Semba K. The mesopontine cholinergic system: a dual role in REM sleep and wakefulness. In: Lydic R, Baghdoyan HA eds. Handbook of behavioral state control: molecular and cellular mechanisms. Boca Raton: CRC 1999: 161-80.
25. Rye DB. Contributions of the pedunculopontine region to normal and altered REM sleep. Sleep 1997;20:757-88.
26. Datta S, Curró-Dossi R, Paré D, Oakson G, Steriade M. Substantia nigra reticulata neurons during sleep-waking states: relation with ponto-geniculo-occipital waves. Brain Res 1991;566:344-7.
27. Takakusaki K, Saitoh K, Harada H, Okumura T, Sakamoto T. Evidence for a role of basal ganglia in the regulation of rapid eye movement sleep by electrical and chemical stimulation for the pedunculopontine tegmental nucleus and the substantia nigra pars reticulata in decerebrate cats. Neuroscience 2004;124:207-20.
28. Bevan MD, Bolam JP. Cholinergic, GABAergic, and glutamate-enriched inputs from the mesopontine tegmentum to the subthalamic nucleus in the rat. J Neurosci 1995;15:7105-20.
29. Hobson JA, Pace-Shott EF. The cognitive neuroscience of sleep: neuronal systems, consciousness and learning. Nat Rev Neurosci 2002;3:679-93.
30. Boraud T, Brown P, Goldberg JA, Graybiel AM, Magill PJ. Oscillations in the basal ganglia: the good, the bad, and the unexpected. In: Bolam JP, Ingham CA, Magill PJ eds. The basal ganglia VIII. Advances in behavioral biology; volume 56. New York: Springer Science and Business Media 2005:3-24.
31. Seijo FJ, Alvarez-Vega MA, Gutierrez JC, Fernandez-Gonzalez F, Lozano B. Complications in subthalamic nucleus stimulation surgery for treatment of Parkinson's disease. Acta Neurochir (Wien) 2007;149:867-75.
32. Fernández-Mendoza J, Lozano B, Seijo F, Fernández-González F, Vela-Bueno A. Subthalamic nucleus activity during human REM sleep: the PGO-like waves [abstract]. J Sleep Res 2006;15:243.
33. Ford B, Winfield L, Pullman SL, et al. Subthalamic nucleus stimulation in advanced Parkinson's disease: blinded assessments at one year follow up. J Neurol Neurosurg Psychiatry 2004;75:1255-9.
34. Ohye C. Depth microelectrode studies. In: Schaltenbrand G, Walker AE, eds. Stereotaxy of the human brain: anatomical, physiological and clinical applications. Stuttgart: Thieme Publishing Group 1982: 372-89.
35. Teijeiro J, Macías RJ, Morales JM, et al. Personal-computer-based system for three-dimensional anatomic-physiological correlations during stereotactic and functional neurosurgery. Stereotact Funct Neurosurg 2000;75:176-87.
36. Yokoyama T, Sugiyama K, Nishizawa S, et al. Neural activity of the subthalamic nucleus in Parkinson's disease patients. Acta Neurochir (Wien) 1998;140:1287-90.
37. Shils JL, Tabliati M, Alterman RL. Neurophysiological monitoring during neurosurgery for movement disorders. In: Deletis V, Shils JL, eds. Neurophysiology in neurosurgery: a modern intraoperative approach. New York: Academic Press 2002: 405-48.
38. Fernández-González F, Seijo F, Menéndez-Guisasola L, et al. Stereotactic target identification for neurosurgery of Parkinson disease. Rev Neurol 1999;28:600-8.
39. Zonenshayn M, Rezai AR, Mogilner AY, Beric A, Sterio D, Kelly PJ. Comparison of anatomic and neurophysiological methods for subthalamic nucleus targeting. Neurosurgery 2000;47:282-92.

40. American Academy of Sleep Medicine. The AASM Manual for the scoring of sleep and associated events. Westchester, IL: American Academy of Sleep Medicine, 2007.
41. Lalo E, Thobois S, Sharott A, et al. Patterns of bidirectional communication between cortex and basal ganglia during movement in patients with Parkinson disease. J Neurosci 2008;28:3008-16.
42. Kühn AA, Williams D, Kupsch A, et al. Event-related beta desynchronization in human subthalamic nucleus correlates with motor performance. Brain 2004;127:735-46.
43. Kühn AA, Doyle L, Pogosyan A, et al. Modulation of beta oscillations in the subthalamic area during motor imagery in Parkinson's disease. Brain 2006;129:695-706.
44. De Cock VC, Vidailhet M, Arnulf I. Sleep disturbances in patients with parkinsonism. Nat Clin Pract Neurol 2008;4:254-66.
45. Vanni-Mercier G, Debilly G. A key role for the caudoventral pontine tegmentum in the simultaneous generation of eye saccades in bursts and associated ponto-geniculo-occipital waves during paradoxical sleep in the cat. Neuroscience 1998; 86:571-85.
46. Hikosaka O, Takikawa Y, Kawagoe R. Role of the basal ganglia in the control of purposive saccadic eye movements. Physiol Rev 2000;80:953-78.
47. Matsumura M, Kojima J, Gardiner TW, Hikosaka O. Visual and oculomotor functions of monkey subthalamic nucleus. J Neurophysiol 1992;67:1615-32.
48. Fawcett AP, Cunic D, Hamani C, et al. Saccade-related potentials recorded from human subthalamic nucleus. Clin Neurophysiol 2007;118:155-63.
49. Vanni-Mercier G, Pelisson D, Goffart L, Sakai K, Jouvet M. Eye saccade dynamics during paradoxical sleep in the cat. Eur J Neurosci 1994;6:1298-306.
50. Wu MF, Mallick BN, Siegel JM. Lateral geniculate spikes, muscle atonia and startle response elicited by auditory stimuli as a function of stimulus parameters and arousal state. Brain Res 1989;499:7-17.
51. Bowker RM, Morrison AR. The PGO spike: an indicator of hyperalertness. In: Koella WP, Levin P. Sleep Research. Basel: Karger 1976:23-7.
52. Hernández-Peón R, Drucker-Colín RR. A neuronographic study of cortico-bulbar hypnogenic pathways. Physiol Behav 1970;5:721-5.
53. Halász P, Terzano M, Parrino L, Bódizs R. The nature of arousal in sleep. J Sleep Res 2004;13:1-23.
54. Llinás R, Ribary U. Coherent 40-Hz oscillation characterizes dream state in humans. Proc Nat Acad Sci U S A 1993;90:2078-81.
55. Steriade M. Corticothalamic resonance, states of vigilance and mentation. Neuroscience 2000;101:243-76.
56. Urrestarazu E, Iriarte J, Alegre M, et al. Beta activity in the subthalamic nucleus during sleep in patients with Parkinson's disease. Mov Disord 2009; 24:254-60.
57. Abe T, Matsuoka T, Ogawa K, Nittono H, Hori T. Gamma band EEG activity is enhanced after the occurrence of rapid eye movement during human REM sleep. Sleep Biol Rhythms 2008;6:26-33.
58. Luppi PH, Gervasoni D, Verret L, et al. Paradoxical (REM) sleep genesis: the switch from an aminergic-cholinergic to a GABAergic-glutamatergic hypothesis. J Physiol Paris 2006;100:271-83.
59. Temel Y, Blokland A, Steinbusch HWM, Visser-Vandewalle V. The functional role of the subthalamic nucleus in cognitive and limbic circuits. Prog Neurobiol 2005;76:393-413.
60. Urbain N, Gervasoni D, Soulière F, et al. Unrelated course of subthalamic nucleus and globus pallidus neuronal activities across vigilance states in the rat. Eur J Neurosci 2000;12:3361-74.
61. Jones BE. Basic mechanisms of sleep-wake state. In: Kryger MH, Roth T, Dement WC, eds. Principles and practice of sleep medicine. 4th ed.. Philadelphia: Elsevier Saunders 2005: 136-53.
62. Maquet P, Smith C, Stickgold R, eds. Sleep and brain plasticity. Oxford: Oxford University Press 2003.
63. Steriade M, McCarley RW. Brain control of wakefulness and sleep. New York: Kluwer Academic/Plenum Publisher 2005.
64. Datta S. Avoidance task training potentiates phasic pontine-wave density in the rat: A mechanism for sleep-dependent plasticity. J Neurosci 2000;20:8607-13.